HHS Public Access

Author manuscript

ACS Chem Neurosci. Author manuscript; available in PMC 2024 January 03.

Published in final edited form as:

ACS Chem Neurosci. 2022 May 18; 13(10): 1534–1548. doi:10.1021/acschemneuro.2c00033.

Effectiveness and relationship between biased and unbiased measures of dopamine release and clearance

Anna C. Everett[1], **Ben E. Graul**[1], **Joakim W. Ronström**[1], **J. Kayden Robinson**[1], **Daniel B. Watts**[1], **Rodrigo A. España**[2], **Cody A. Siciliano**[3], **Jordan T. Yorgason**[*,1]

[1]Brigham Young University, Department of Cellular Biology and Physiology, Provo, UT 84602, USA

[2]Drexel University, Department of Neurobiology & Anatomy, Philadelphia, PA 28619, USA

[3]Vanderbilt University, Center for Addiction Research, Nashville, TN 37203, USA

Abstract

Fast-scan cyclic voltammetry (FSCV) is an effective tool for measuring dopamine release and clearance throughout the brain, especially the striatum where dopamine terminals are abundant and signals heavily regulated by release machinery and the dopamine transporter (DAT). Peak height is perhaps the most common method for measuring dopamine release but is influenced by changes in clearance. Michaelis-Menten based modeling has been a standard in measuring dopamine clearance, but is problematic in that it requires experimenter fitted modeling subject to experimenter bias. The current study presents the use of the first derivative (velocity) of evoked dopamine signals as an alternative approach for measuring and distinguishing dopamine release from clearance. Maximal upwards velocity predicts reductions in dopamine peak height due to D_2 and $GABA_B$ receptor stimulation and by alterations in calcium concentrations. The Michaelis-Menten maximal velocity (V_{max}) measure, an approximation for DAT levels, predicts maximal downward velocity in slices and *in vivo*. Dopamine peak height and upward velocity were similar between wildtype and DAT knock out (DATKO) mice. In contrast, downward velocity was lower, and exponential decay (tau) was higher in DATKO mice, supporting use of both measures for extreme changes in DAT activity. In slices, the competitive DAT inhibitors cocaine, PTT and WF23 increased peak height and upward velocity differentially across increasing concentrations, with PTT and cocaine reducing these measures at high concentrations. Downward velocity and tau values decreased and increased respectively across concentrations, with greater potency and efficacy observed with WF23 and PTT. *In vivo* recordings demonstrated similar effects of WF23, PTT, and cocaine on measures of release and clearance. Tau was a more sensitive measure at low concentrations, supporting its use as a surrogate for the Michaelis-Menten measure of apparent

[*]Corresponding Author: jordanyorg@byu.edu.

Author Contributions:

ACE, RAE, CAS and JTY designed experiments and performed the research. ACE, BEG, DBW, JKR and JTY analyzed and interpreted experiments. JTY wrote additional software for analysis. ACE, BEG, JWR and JTY contributed to manuscript writing.

Conflicts of Interest: The authors declare no competing financial interest.

Supporting Information: Comparison between upward velocity and Michaelis-Menten Vmax. Comparison between downward velocity and exponential decay (tau). Both comparisons are made with slice and in vivo data.

affinity (K_m). Together, these results inform on the use of these various measures for dopamine release and clearance.

Keywords

dopamine; dopamine transporter; fast scan cyclic voltammetry; Michaelis-Menten; kinetics; striatum

Introduction

Fast-scan cyclic voltammetry (FSCV) is a widely used electrochemical detection technique that can be highly selective for specific analytes. This technique is perhaps most frequently used for detection of monoamines (such as dopamine) and indolamines 1, but is also increasingly used for detecting other neurotransmitters such as hydrogen peroxide and purines[2, 3]. FSCV has good temporal resolution and chemical specificity, making it an ideal tool for studying the mechanisms underlying rapid neurotransmitter release and clearance. For the past 30 years, the Michaelis-Menten model has been used alongside voltammetry techniques to study the kinetics of the dopamine transporter (DAT)[4–7]. In general, the Michaelis-Menten equation is used to measure first order enzymatic kinetics, solute binding efficiency, and enzyme concentrations 8. The maximal rate of dopamine uptake is a measure of DAT levels and identified as V_{max} and dopamine's apparent binding affinity for the DAT is the Michaelis-Menten constant (K_m).

The voltammetry modified version of this model was described previously[5–7] and includes the typical V_{max} and K_m variables. The following modified Michaelis-Menten equation is commonly used to determine changes in release and DAT function.

$$\frac{d[DA]}{dt} = f[DA_p] - \frac{V_{max}}{\left(\left(\left[\frac{K_m}{[DA]}\right]\right) + 1\right)}$$

This equation models the change in evoked extracellular dopamine signal ([DA]) from the presynaptic terminal across time, taking into account the frequency f of the stimulating pulse, amount released per pulse (release rate constant, [DA_p]), the maximal rate of dopamine uptake (V_{max}), and the apparent binding affinity of dopamine for the DAT (K_m). This equation makes several assumptions about the dopamine signal, such as a fixed amount of dopamine released per stimulation pulse, large enough signal that DAT transporters in the vicinity are saturated, and that the primary mechanism for clearing dopamine is through the DAT (as opposed to diffusion or another transporter). One additional variable is included in this model is the thickness layer, which is a deconvolution factor used as a correction coefficient for improving model fit[5, 6].

The process for analyzing voltammetry data using these kinetic parameters is complicated and not completely standardized. Using the concentration vs. time trace at the peak dopamine oxidation potential, data are imported into specialized software that allows for user defined control over values from the model. The values are manually[6, 9–11] or

semi-automatically adjusted (e.g., using simplex fitting) 7. A second simulated curve is superimposed on the original, and correlation values are displayed so that the user can determine the fit of the curve. Having the curve fit by a computer algorithm reduces the experimenter bias, but can also be highly sensitive to noise 7. Each of these methods allows for constraint of specific variables, which allows for hypothesis driven modeling. One method for analysis is to have all the values adjusted (non-constrained) until a curve is fit 12. Another common method is to start off with a specific fixed value for K_m (e.g., 160–200 nM based on previous dopamine binding studies 13). With this fixed K_m value, only the thickness layer, release concentration, and V_{max} are adjusted to determine baseline release and clearance values[14–17]. This second method is often combined with a third approach where the V_{max} is constrained after drug application, and K_m becomes variable in the presence of psychostimulants[17–20].

Although the use of these approaches has been effective at teasing out important physiological and pharmacological effects, choosing what values to constrain is at the discretion of the experimenter, resulting in an inherent experimenter bias. The overall strength of the fit can be determined by the Spearman's rank correlation coefficient 6. However, the resulting V_{max} and K_m values can vary greatly depending on the constraints introduced by the experimenter performing the curve fitting. There are other methods that do not rely on experimental-fitted models, such as computerized nonlinear regression 7. However, these methods still rely on experimenter input on model constraints. As an alternative method, we showed previously that the exponential decay value tau strongly relates to changes in apparent K_m (in the presence of psychostimulants) 6. In contrast, V_{max} did not correlate well with exponential decay measures 6. Thus, the present work examines alternative methods for studying dopamine release and clearance kinetics involving the first derivative, or velocity, which is an easily replicable measure of slope across a time domain-based signal. Velocity values are compared across conditions known to influence dopamine release and clearance and compared to Michaelis-Menten model-based measures of V_{max} from slice and *in vivo* preparations. Unlike the Michaelis-Menten model, these analytical measures are not dependent on enzymatic activity, making them ideal for describing clearance in animal models that do not contain transporters. The present work describes this use of easily measurable values of slope that have reduced analytical bias and may inform on applications for studying dopamine clearance via the DAT, as well as diffusion and other non-DAT-mediated dopamine clearance.

Results and Discussion

Upward velocity and peak height as measures of changes in dopamine release

In order to establish alternate measures of dopamine release, the maximal upwards velocity was examined under conditions that alter release probability. The release curve and first derivative of an evoked dopamine signal (1 pulse) are shown (Figure 1A). Dopamine release was examined before and after activation of two inhibitory G_i-protein coupled receptors (GPCRs), $GABA_B$, and D_2 inhibitory receptors (Figure 1B–C). A maximal concentration of the $GABA_B$ agonist baclofen (30 μM) reduced NAc dopamine peak height by 30.1%, which reversed upon antagonist application (CGP55845; 200 nM). The D2 agonist quinpirole (1

μM) reduced dopamine release to a much greater extent (92.7%), which similarly reversed with D2 antagonist application (sulpiride; 600 nM). Peak height and velocity up strongly correlated in these experiments (Figure 1C; n = 35 samples from 5 mice, r = 0.999, slope = 5.006 ± 0.008, $p < 0.001$). Michaelis-Menten V_{max} correlates to velocity up (Figure 1D; n = 35 sample from 5 mice, r = 0.7, slope = 1.99*x ± 0.35, $p < 0.001$) and to velocity down (Figure 1E; n = 35 sample from 5 mice, r = 0.84, slope = −0.89*x ± 0.099, $p < 0.001$).

Electrically evoked dopamine release is calcium dependent[21, 22] and dopamine release at physiological calcium (~1.2 mM) levels is ~50% of release observed from maximal (2.4–4.8 mM) calcium concentrations 23. Therefore, the effects of calcium (1.2–4.8 mM) on evoked dopamine release (20Hz, 5p) were compared between peak height and upward velocity measures (Figure 2). Experiments with higher calcium (2.4–4.8 mM) concentrations exhibited ~232% greater dopamine release (200% for 2.4 mM, 263% for 4.8 mM) than physiological (1.2 mM) calcium levels (Figure 2A–B; One-way ANOVA, $n_{1.2} = 6$ slices, $n_{2.4} = 10$ slices, $n_{4.8} = 4$ slices, $F_{2,17} = 13.65$, $p < 0.001$). A Tukey's HSD posttest revealed significantly increased dopamine release differences between calcium concentrations (1.2 to 2.4 mM: $p < 0.01$, q = 6.238; 1.2 to 4.8 mM: $p < 0.001$, q = 6.549). Increasing calcium beyond standard FSCV concentration (from 2.4 mM to 4.8 mM) did not significantly increase dopamine release ($p > 0.05$, q = 1.7). Peak height correlated across increasing calcium concentrations for upward velocity (Figure 2C; n = 20, r = 0.888, slope = 0.286 ± 0.0349, $p < 0.001$). This correlation was not as strong as that observed with baclofen and quinpirole experiments, possibly due to the use of multiple pulse stimulations, which may increase variability due to recruitment of additional feedback mechanisms. Thus, from GPCR-mediated inhibition experiments, and calcium dependent release experiments, there is a clear relationship between release peak height and the upward velocity of release. This is not surprising since velocity simply and effectively quantifies the rising slope of an existing curve. Changes in the relationship between upward velocity and peak would only be expected if there were very large increases in peak height associated with decreased dopamine clearance, resulting in an overall decreased upward velocity. This idea is investigated later with psychostimulant application in slices.

Similar to the previous experiments, the Michaelis-Menten V_{max} correlates with velocity up (Figure 2D; n = 20, r = 0.676, slope = 0.145*x ± 0.041, $p = 0.003$). More relevant to its value as a measure up dopamine uptake, V_{max} correlates strongly with velocity down (Figure 2E; n = 20, r = 0.845, slope = −0.658*x ± 0.108, $p < 0.001$). As evidence for velocity down working as a surrogate for V_{max}, voltammetry data were modeled using the described Michaelis-Menten approach, substituting velocity down for V_{max}, and solving for DAp and K_m values. Signals where velocity down was substituted for V_{max} consistently correlated with fitted models (n=16, mean spearman r = 0.94 ± 0.015). This method of fixing V_{max} produced a mean K_m of 200.2 ± 11.93 nM which is in the range of K_m values used by others 7. Three signals fit using this approach, and resulting simulated curves, are demonstrated (Figure 2F) with examples from each calcium concentration. The subsequent experiments further explore downward velocity as a measure of dopamine clearance.

Downward velocity as a measure of dopamine transporter function

The predictive value of maximal downwards velocity was investigated in relation to the Michaelis-Menten value V_{max}—an analytical value indicative of the maximal rate of dopamine clearance mediated by the DAT[4, 6]. The Michaelis-Menten V_{max} measure was obtained under baseline (non-drug) conditions in brain slices (*ex vivo*; Figure 3A–C) and in anesthetized mice (*in vivo*; Figure 3D–F). The traces of evoked dopamine release (1 pulse) and first derivatives with low (blue) and high (green) downward velocity values from *ex vivo* recordings are shown (Figure 3A). Maximal downward velocity and Michaelis-Menten V_{max} values in brain slices are correlated (Figure 3B; n = 8 slices, r = 0.79, slope = −0.158 ± 0.05, $p = 0.02$). *In vivo* evoked (60 Hz, 30 pulses) dopamine release traces with low (orange) and high (pink) downward velocity rates are shown (Figure 3D). From *in vivo* experiments, downward velocity values correlated with Michaelis-Menten V_{max} values (Figure 3E; n = 9 mice, r = 0.819, slope = −0.844 ± 0.224, $p = 0.007$). Michaelis-Menten V_{max} values from these experiments in slice were much larger than *in vivo* values (*ex vivo*: 2.463 ± 0.472; *in vivo*: 1.025 ± 0.094 μM/s; Two tailed t-test: $t_{16} = 2.987$, $p = 0.009$). In contrast, downward velocity values covered a similar range and were thus more comparable between *in vivo* and *ex vivo* conditions, though there were significant differences between downward velocity values under the two conditions (*ex vivo*: −1.059 ± 0.095; *in vivo*: −0.698 ± 0.084 μM/s; Two tailed t-test: $t_{14} = -2.472$, $p = 0.027$). The source of this variability between preparations is unknown, but may reflect inherent differences in recording conditions (e.g., stimulation settings, extracellular conditions) making it difficult to compare across preparations. Interestingly, the relationship between upwards velocity and V_{max} that exists under G_i stimulation and varying calcium conditions does not exist in normal baseline conditions (Supporting Information Figure 1A, *ex vivo*: n = 8 slices, r = 0.208, slope = 0.364 ± 0.698, $p = 0.621$; Supporting Information 1C, *in vivo*: n = 8 slices, r = 0.528, slope = 1.058 ± 0.643, $p = 0.144$). This suggests that upwards velocity is a better predictor when there are large changes in V_{max} as opposed to the small differences in V_{max} that may exist between subjects.

The exponential decay constant tau is a simple and commonly used method for describing dopamine uptake kinetics 6. Thus, tau was compared to Michaelis-Menten V_{max} (Figure 3C, F) and downward velocity (Supporting Information Figure 1B, D) values *ex vivo* and *in vivo*. Tau was not significantly correlated with V_{max} (n = 9 mice, r = 0.372, slope = −2.227 ± 2.098, $p = 0.324$) or maximal velocity down (n = 8 slices, r = 0.516, slope = −0.139 ± 0.094, $p = 0.19$). Thus, while previous studies show that tau is effective for measuring general changes in dopamine uptake and correlates with the Michaelis-Menten K_m, it is not a suitable replacement for V_{max}. This is consistent with our previous comparison 6. These data support the idea that tau and downward measure fundamentally different processes, and suggests that both measures of uptake are useful for determining changes to the multifaceted process. For the remaining experiments, peak, upwards velocity, downwards velocity and tau will be explored in the context of genetic and pharmacological DAT inactivation.

Downward velocity as a measure of dopamine clearance in DAT knockout mice

Peak height and downward velocity measures were examined in DATKO mice to determine how much the DAT contributes to these measures (Figure 4). Since downward velocity

is an effective predictor at measuring DAT function in relation to the Michaelis-Menten V_{max} measure, it was expected that this measure would be most affected by DAT removal. Furthermore, Michaelis-Menten parameters cannot be tested in DATKO mice due to violation of modeling parameters from complete lack of DAT enzymatic activity 5. Dopamine signals were examined at three stimulation conditions which produce varying dopamine release concentrations (1 pulse, 5 pulses at 20Hz, 24 pulses at 60Hz). Example dopamine release (Figure 4A) and velocity (Figure 4B) traces are shown. Upwards velocity positively correlated with peak height in WT mice (velocity: n = 46, r = 0.838, $p <$ 0.001, slope = 1.92 ± 0.19) and in DATKO mice (velocity: n = 36, r = 0.801, $p <$ 0.001, slope = 1.59 ± 0.2). The relationship between peak dopamine and upward velocity (across stimulation conditions) was examined, and no significant difference was observed between WT and DATKO mice ($F_{1,78} = 1.38$, $p = 0.243$). Therefore, peak dopamine signals from multiple pulse stimulations relate to maximal upward velocity measures, and this relationship is maintained in the absence of the dopamine transporter. Two-way repeated measures ANOVA for peak release (Figure 4C) revealed a main effect of stimulation intensity ($F_{2,56} = 186.74$, $p < 0.001$), but no effect of mouse strain ($F_{1,56} = 2.65$, $p =$ 0.115) and no significant interaction ($F_{2,56} = 1.25$, $p = 0.294$). For upward velocity (Figure 4D–E) there was a main effect of stimulation intensity ($F_{2,56} = 68.48$, $p < 0.001$), but no effect of mouse strain ($F_{1,56} = 0.70$, $p = 0.408$) and no significant interaction between these terms ($F_{2,56} = 0.27$, $p = 0.766$). Thus, detection of release as measured by peak and upward velocity is increased with higher stimulation intensities and is similar between WT and DATKO mice.

Dopamine clearance was evaluated using striatal slices from WT and DATKO mice (Figure 5). Average (±SEM) first derivative curves across an evoked release time course are shown (Figure 5A; 20 Hz, 5 pulse stimulation). There are clear differences in overlap for the downward velocity slope in these two strains. A subtraction between average dopamine velocity curves from WT and DATKO mice across stimulation conditions highlights the time course of velocity differences (Figure 5B). Interestingly, greater downward velocities were observed with higher stimulation intensity (compare green 5 pulse curve to black 1 pulse curve in Figure 5B), with greatest velocities observed in WT mice at the 60Hz 24 pulse stimulation conditions (WT 1p: −1.395 μM/s; WT 20Hz5p: −1.963 μM/s; WT 60Hz24p: −2.138 μM/s). Not surprisingly, longer duration stimulations also resulted in subtraction curves with longer duration downward velocities. These results show that DAT effects across time can be more pronounced with longer stimulations. Maximal downward velocity values across stimulation conditions and strains are shown (Figure 5C). Two-way repeated measures ANOVA for downwards velocity revealed a main effect of stimulation intensity ($F_{2,56} = 23.27$, $p < 0.001$) and mouse strain ($F_{1,56} = 12.33$, $p = 0.002$), but no significant interaction between these terms ($F_{2,56} = 1.58$, $p = 0.215$). Two-way repeated measured ANOVA for tau revealed a main effect of mouse strain ($F_{1,56} = 58.13$, $p < 0.001$), but no significant main effect of stimulation intensity ($F_{2,56} = 1.93$, $p = 0.155$) nor a significant interaction between these terms ($F_{2,56} = 1.00$, $p = 0.376$). These DATKO experiments highlight the utility of downward velocity for measuring large changes in dopamine uptake by complete removal of the DAT. While tau can measure drastic differences between mouse

strains, it is not as sensitive as downwards velocity for measuring changes in rapid uptake related to stimulation intensity.

Dopamine transporter blockers differential effects on release and uptake

Dopamine transporter inhibitors of the tropane family share a DAT binding site with dopamine[24–26]. Therefore, it is expected that due to competition effects, downward velocity will have varying sensitivity to DAT inhibitors that will be weakest at lowest concentrations and strongest with inhibitors with higher affinity. The effects of tropane DAT competitive blockers with varying affinities (WF23, PTT, Cocaine) on dopamine clearance was measured *ex vivo* (Figure 6). Representative release traces are shown for WF23 (Figure 6A), PTT (Figure 6B) and cocaine (Figure 6C). The highly potent WF23 (K_i = 0.1 nM) 27 elevated peak height (Figure 6D) across increasing concentrations (10 nM-3 μM), with greatest increases observed at the 300 nM concentration at ~458% of baseline. Similarly, PTT (K_i = 3 – 8.2 nM; 100 nM – 30 μM)[28, 29] increased peak height with greatest effects at 1 μM (~282% of baseline). Cocaine (Ki = 120 – 189 nM; 300 nM- 30 μM)[30, 31] elevated peak height to a maximum of ~134% baseline at 1–3 μM. Uniquely, cocaine also decreased signals by ~49% from baseline at 30 μM. Although WF23 and PTT both exhibited an inverted U-shaped curve, peak height never fell below baseline levels for these drugs. Two-way ANOVA on peak height data revealed a main effect of concentration ($F_{8,60}$ = 6.28, p < 0.001), but indicated no drug effect ($F_{2,60}$ = 0.06, p = 0.942 or interaction ($F_{1,60}$=1.51, p = 0.126).

The upward velocity measures were affected differently than peak height by competitive DAT inhibitors. The greatest effects for upward velocity across the three drugs were at 100 nM for WF23 (~194%) and 300 nM concentrations for PTT (~112%) and cocaine (~118%; Figure 6E). Upward velocity reduced below baseline at >1 μM (WF23, PTT) and >10 μM (cocaine) concentrations. This is an important example where increases in peak height do not relate directly to upward velocity and suggests that the increase in peak height observed at the higher concentrations of inhibitors is likely due to a different mechanism, such as increased spread from distant dopamine terminals. This phenomenon can be observed in traces from WF23 and PTT experiments at high concentrations, where the peak height is larger than the baseline, and the time for that peak is delayed (rightward shifted), reflecting a slower upward velocity (Figure 6A–B). Two-way ANOVA on upward velocity data revealed a main effect of concentration ($F_{8,60}$ = 4.19, p < 0.001), no drug effect ($F_{2,60}$ = 0.73, p = 0.45), and no interaction ($F_{1,60}$ = 1.20, p = 0.291).

Since the association between upward velocity and peak height is weaker in the presence of high concentrations of DAT blockers, this measure may be particularly useful in dissociating and interpreting mechanisms underlying increases in peak height that are not due to increased vesicular fusion. The ratio between upward velocity and peak height was examined across drug concentrations (Figure 6F) and exhibited a clear decrease for all DAT blockers, with greater efficacy and potency for WF23 and PTT over cocaine. Two-way ANOVA on the ratio between upward velocity and peak height data revealed a main effect of concentration ($F_{8,60}$ = 70.35, p < 0.001), a main effect of drug ($F_{2,60}$ = 12.16, p = 0.001), and a significant interaction ($F_{1,60}$ = 8.45, p < 0.001).

The effects of tropane analogs on downward velocity in striatal slices was examined next (Figure 7). First derivative traces are shown for WF23, PTT and cocaine (Figure 7A–C). All three drugs reduced downward velocity at high concentrations (Figure 7D), but effects were mixed at low (<100 nM) concentrations, with WF23 in some experiments exhibiting faster (more negative) downward velocity (see example traces in Figure 7A). Therefore, WF23 effects were examined with (Figure 7D) and without (**inset**) experiments where velocity increased at low concentration ranges. For WF23 and PTT experiments, downward velocity was reduced for a similar range of concentrations (>100 nM), which was leftward shifted from cocaine, reflective of the increased potency of WF23 and PTT for the DAT over cocaine. Cocaine effects were modest (apparent effects at >1 μM) and did not plateau until ≥30 μM. These data suggest that downward velocity is an effective tool for measuring relative potency for competitive DAT inhibitors.

The Michaelis-Menten K_m is frequently used for describing effects of DAT inhibitors[19, 20, 32, 33] and correlates strongly with the exponential decay measure tau 6. Therefore, in order to establish the relationship between exponential decay and downward velocity, the effects of tropane analogs on tau were examined (Figure 7E). Tau was more sensitive to tropane analogs than downward velocity, with WF23 increasing tau with the greatest efficacy and potency ($LogEC_{50}$ = 0.242), followed by PTT ($LogEC_{50}$ = 2.326) and cocaine ($LogEC_{50}$ = 12.59). Two-way ANOVA on tau data revealed a main effect of concentration ($F_{8,60}$ = 13.90, $p < 0.001$) and a significant interaction between these terms ($F_{16,60}$ = 4.69, p <0.001), but no main effect of drug ($F_{2,60}$ = 2.51, p = 0.12). Considering the increased sensitivity of tau over downward velocity in measures of psychostimulant sensitivity, downward velocity appears more effective at measuring changes in dopamine uptake reflective of changes in transporter numbers (similar to V_{max}), while tau appears more effective for detecting changes in apparent affinity of dopamine for the DAT (similar to K_m).

Decreases in the upward velocity to peak height ratio (seen in Figure 6F) may be due to reduced dopamine clearance. Since tau is a sensitive measure of impaired clearance for competitive inhibition (Figure 7E), the relationship between these two values was examined. Upward velocity to peak ratio correlated to tau (Figure 7F) for WF23 (Spearman r = −0.82, $p < 0.001$) and PTT (Spearman r = −0.862, $p < 0.001$) and significantly, but less for cocaine (Spearman r = −0.3802, p = 0.0077), likely reflecting cocaine's lower efficacy at reducing the upward velocity to peak height ratio and lower efficacy on increasing tau. These data highlight the relationship between increases in dopamine signals and decreases in uptake which are most apparent as tau increases but are different for each competitive inhibitor. The relationship between tau and downward velocity was further examined in the context of DAT inhibitors (Figure 7G). Tau values significantly correlated with downward velocity for WF23 (Spearman r = 0.784, $p < 0.001$) PTT (Spearman r = 0.894, $p < 0.001$) and cocaine (Spearman r = 0.652, $p < 0.001$), and tau was most strongly related at smaller downward velocities. Therefore, reductions in upward velocity to peak ratio are due in part to impaired clearance, and tau becomes more predictive of downward velocity in conditions where dopamine clearance is severely impaired by reuptake inhibitors.

The effects of potent competitive DAT inhibitors (WF23 and PTT) and a less potent inhibitor (cocaine) were tested *in vivo* in order to establish a measure of sensitivity for these three different drugs. Experiments were performed across a 30-minute time course, and measures of peak height, upward velocity, downward velocity, and tau were all examined (Figure 8). To compare the effect of each drug, one-way ANOVAs were conducted at the peak effect of each measure. Peak height was significantly different between WF23, PTT, and cocaine with a much larger increase in WF23 and PTT in comparison to cocaine (Figure 8A: One-way ANOVA; $F_{2,17} = 4.49$, $p = 0.027$). Upwards velocity was trending towards significance with slightly higher velocity values using WF23 and PTT (Figure 8A **Inset**: One-way ANOVA; $F_{2,17} = 3.011$, $p = 0.076$). However, when we compared the ratio of upwards velocity to peak height, there was a strong significant difference across the three drugs (Figure 8B: One-way ANOVA; $F_{2,17} = 11.338$, $p = 0.000744$). Tau was much higher in WF23 in comparison to PTT, and tau was higher in PTT than cocaine (Figure 8C: One-way ANOVA; $F_{2,16} = 8.7629$, $p = 0.00269$). The upward velocity to peak ratio correlated with changes in tau (Figure 8D) for WF23 (Spearman r = −0.606, $p < 0.001$) and PTT (Spearman r = −0.938, $p < 0.001$), but did not correlate with cocaine (Spearman r = −0.099, p = 0.333). However, there was no significant difference in downwards velocity between drugs, and quite a lot of variability (Figure 8E: One-way ANOVA; $F_{2,17} = 1.892$, $p = 0.181$). Interestingly, in some WF23, PTT, and cocaine experiments the downward velocity increased initially (Figure 8E; during the first 20 minutes; Two-way RM-ANOVA; Time effect: $F_{12,68} = 1.57$, $p = 0.12$; Drug effect: $F_{1,68} = 0.41$, $p = 0.544$; Interaction: $F_{12,68} = 0.49$, $p = 0.091$), likely due to initial low concentration effects on increasing DAT activity which were also observed in slices (Figure 7A, D). When these increasing values are removed, there is a clear decrease in downward velocity induced by WF23, PTT, and cocaine at the 5 second time points, with effects ordered by drug potency (Figure 8E **Inset**; Two-way RM-ANOVA; Time effect: $F_{12,20} = 3.4$, $p = 0.008$; Drug effect: $F_{1,20} = 1.24$, $p = 0.381$; Interaction: $F_{12,20} = 0.45$, $p = 0.92$). Similar to slice experiments, downward velocity from *in vivo* experiments correlated with tau (Figure 8F) for WF23 (Spearman r = 0.688, $p < 0.001$), PTT (Spearman r = 0.244, $p = 0.007$), and cocaine (Spearman r = 0.659, $p < 0.001$).

The present experiments examine measures of dopamine release and clearance. Dopamine peak height is reduced by application of $GABA_B$ and D_2 agonists and increased with enhanced calcium levels and greater stimulation intensity. This release measure correlated strongly with maximal upward velocity. Maximal downward velocity correlated with the Michaelis-Menten uptake measure of V_{max}, an indirect measure of DAT expression, whereas the exponential decay measure tau related more to the Michaelis-Menten measure K_m. Genetic and pharmacological blockade of the DAT resulted in concentration dependent reductions in the observed maximal downward velocity and increases in tau, with greatest sensitivity in the tau measure. The application of these measures to dopamine signals introduces an unbiased approach for measuring release and clearance, which is needed for improving analysis standardization across the field.

The relationship between drug induced changes in peak height and upwards velocity is complex and represents a concert between cellular mechanisms underlying release and clearance. In conditions where release is solely influenced, increases in peak height

are tightly related to velocity increases. In contrast, for tropane concentration response experiments, peak height increased across drug concentrations, but the velocity of the rising peak varied greatly in a drug and concentration dependent manner (increasing at low and decreasing at high concentrations respectively). Peak height increases associated with slower upward velocities indicate the crude nature of peak height as a measure of release alone. The dissociation between these measures apparent in the presence of DAT blockers is indicative of the multitude of effects of these drugs on dopamine terminal function.

The modified voltammetry Michaelis-Menten model is used to calculate the amount of dopamine released ([DAp]) in the context of DAT enzymatic activity values (V_{max} and K_m) 5. This same model was previously used to measure cocaine's DAT-blocking effects and comparisons were made across dopamine signal peak height, [DAp], K_m and the area under the curve 6. From these previous experiments, peak height correlated strongly with [DAp] ($r = 0.97$) across cocaine concentrations (300 nM- 30 μM). Presently, similar increases in peak height were observed across concentrations of DAT blockers, with increases above baseline for most concentrations, and slight reductions in dopamine peak with cocaine at 30 μM (reduced by ~20%). As a comparison, upward velocity increased at concentrations ≤ 1 μM for WF23/PTT (peak increases of ~32–57% at 300 nM respectively) and ≤ 3 μM for cocaine (peak increases of ~33% at 300 nM). In contrast, upward velocity decreased at higher concentrations (~18% decreases with WF23 at 3 μM; ~33–42% decreases with PTT at 10–30 μM; ~13–48% decreases with cocaine at 10–30 μM). Together with our previous study, these data suggest that the [DAp] and dopamine peak height are not completely reflective of release, and interpretation is heavily influenced by reduced uptake, where peak height increases but upward velocity does not. In experiments where PTT and WF23 were applied, peak dopamine release was increased over baseline values across concentrations, but with reduced upward velocity in the 3–30 μM range. This concentration range coincided with larger reductions in downward velocity. This suggests that the decrease in upwards velocity, but overall increase in peak, is due to increased detection of release from diffusion from distant compartments. In contrast to DAT blocker experiments, there were similar upward velocities observed between WT and DATKO mice. This finding was surprising because DATKO mice have been heavily used as a comparison group for studying clearance kinetics in the absence of the DAT (i.e. diffusion)[34, 35] and suggests that there are compensations in DATKO mice affecting release and potentially clearance. Therefore, experiments examining dopamine diffusion may benefit more from using these or other high affinity DAT blockers. These results also support an unknown adaptation in dopamine clearance—possibly secondary clearance mediated by the cholesterol sensitive organic cation transporter 36.

The diversity of observed effects of DAT inhibitors on peak height and velocity measures of release across concentrations are indicative of the multiple effects of DAT inhibitors on dopamine terminals. One of the mechanisms recruited during DAT blockade is activation of dopamine D_2 type receptors 37. Dopamine D_2-type receptors are inhibitory GPCRs, located on presynaptic dopamine terminals (as autoreceptors) and on postsynaptic neurons (as heteroreceptors) in the striatum. At the soma, D_2 autoreceptors activate inhibitory effectors, including the G-protein-coupled inward rectifying potassium (GIRK) channels, to drive membrane hyperpolarization 38. In vivo, cocaine increases dopamine levels 39,

resulting in D_2 mediated inhibition of somatic activity 40. In a slice, evoked dopamine release is insensitive to D_2 antagonists[41, 42], demonstrating that extracellular tone is minimal in slice conditions. Fast-scan controlled adsorption voltammetry (FSCAV) studies in slices have reported extracellular dopamine levels of ~11 nM in the striatum 43 and ~40 nM in the SNc 44. Bath application of cocaine (10 μM) increased extracellular dopamine in the SNc by ~6.8 nM 44. There are currently no FSCAV reports on dopamine levels after cocaine in striatal slices. However, bath application of dopamine (1 μM) produces modest (~5–10%) activation of D_2 receptors (IC50 of 36 μM), and cocaine (10 μM) quadruples D_2 sensitivity (IC50 at 9 μM) 45. Several studies have shown D_2 mediated inhibition of dopamine release with cocaine at high concentrations (10 μM) 46 47. We have observed D_2 mediated inhibition of dopamine release by cocaine at concentrations as low as 1 μM 48. At low concentrations insufficient for inhibiting uptake (10 nM), cocaine has been shown to enhance D_2 receptor stimulation possibly due to positive allosteric effects on D_2 receptors[49–51]. Blocking D_2 receptors in the presence of cocaine (1–10 μM) results in greater dopamine release[46–48]. Since reductions in dopamine release velocity were observed herein in the presence of the D_2 agonist quinpirole, and since DAT blockers examined are known to increase D_2 activation, the decrease in velocity observed with DAT blockers can be attributed in part to D_2 autoreceptor activation. In terminals, D_2 activation will likely influence several effectors to attenuate dopamine release, including activation of Kv2.1 channels 52, inhibition of snare proteins 53 and inhibition of synthesis proteins (i.e. tyrosine hydroxylase) 54. It is unknown if $GABA_B$ receptors recruit this same machinery at dopamine terminals, or if some of cocaine's effects are through enhancement of $GABA_B$ effects. It seems likely that adaptations from cocaine would affect $GABA_B$ sensitivity considering the overlap in effector coupling for these receptors 55. Cholinergic interneurons (CINs) are a major regulator of dopamine activity, and electrically evoked dopamine release is initiated in part through release of acetylcholine and subsequent depolarization through activation of nicotinic acetylcholine receptors (nAChRs)[48, 56]. Furthermore, nAChR allosteric activators and nAChR blockers enhance and reduce dopamine release respectively[48, 57]. Also, the dopamine release process is dependent on sodium channel mediated depolarization on dopamine terminals 48, subsequent opening of voltage gated calcium channels 58 and calcium entry, which interact with snare proteins to trigger vesicular fusion 59. Cocaine has been shown to block nAChR conductance at concentrations > 3 μM 60. Mice lacking the β-2 nAChR subunit have reduced sensitivity to inhibition from cocaine 60. In this latter study, peak reductions still occurred in β-2 knockout mice, but with a considerable reduction in sensitivity. Indeed, attenuated increases were observed in WT mice at concentrations > 2 μM concentrations, but in β-2 knockouts only at concentrations > 10 μM 60. The inhibition observed at higher concentrations in β-2 knockout mice was attributed to cocaine's well-known anesthetic effect 60. Since WF23 and PTT share some structural homology with cocaine, it is likely that these drugs are acting through these several mechanisms to attenuate release. However, whether WF23 and PTT have nAChR or anesthetic effects at the tested concentrations remains unknown.

The downward velocity measure was highly indicative of DAT function. Downward velocity significantly correlated with Michaelis-Menten V_{max} values *in vivo* and in slice in WT mice and was considerably reduced in DATKO mice. Furthermore, downward velocity decreased

after application of DAT blockers in slice and *in vivo*. Thus, downward velocity reliably predicts slower DAT kinetics in the presence of blockers. Since DATKO mice have no enzymatic function, the Michaelis-Menten V_{max} cannot be used in DATKO analysis. This highlights an important utility of downward velocity in studying dopamine clearance without violating specific enzymatic conditions.

Although data in the present study indicate a clearance mechanism mainly mediated through the DAT, other mechanisms are also involved in clearance. Data from DATKO mice and pharmacological DAT blockade experiments presented herein indicate multiple aspects of dopamine transmission (release and clearance) that are altered under these conditions. Both velocity down and tau measures are slowed in these conditions. Interestingly, with increased stimulation intensity, dopamine clearance rate in DATKO slices was increased, suggesting additional recruited mechanisms of clearance. Interestingly, the organic cation transporter 3 (OCT3) has been implicated in catecholamine clearance in the striatum 61 and basolateral amygdala 62. DATKO mice have previously been used as a model of diffusion, but recent evidence demonstrates that OCT3 is active and even upregulated in DATKO transgenic rats 63. While not tested exclusively herein, it is possible that increased stimulation intensity is recruiting this alternate uptake mechanism. Interestingly, peak height was consistently increased with DAT blockade at low concentrations. This increase in peak height has been observed many times previously, and is attributed to either facilitated release 64 or increased rate of diffusion, resulting in bigger peaks[22, 65]. With peak height increasing, we largely saw increased upward velocity with low concentrations of DAT inhibitors, and most robustly with WF-23. The ratio between upward velocity and peak height starts to decrease with higher concentrations, which may be more indicative of increased rate of diffusion due to fewer active DAT sites. Others have reported increased peak height with slower time to peak in the presence of DAT inhibitors, which is attributed and supportive of this measure as one of increased diffusion[22, 65, 66]. Importantly, dextran, which is known to slow diffusion rate, also results in increases in peak height in areas where diffusion is a major clearing mechanism 65.

Other factors can also affect diffusion. The tortuosity of the slice, determined by synaptic and extrasynaptic organization, is a major factor in diffusion and has been shown to be altered in disease states 67. Whether diffusion is altered in DATKO animals is unknown. Interestingly, we observed similar peak heights between WT and DATKO animals, suggesting similar release. This is surprising since previous studies have observed reduced release in DATKO mice[68, 69]. Interestingly, other recent research has shown increased release in DATKO compared to WT rats 63, and others have shown no difference 70. There were no obvious differences in methods to account for these discrepancies. Indeed, the original studies are missing important information (e.g. stimulation intensity, ACSF composition, animal age, etc) that may contribute to release differences. In speculation, it seems possible that removing the primary mechanism of dopamine clearance from an animal would result in age specific developmental alterations that are observed in some studies but not others.

Dopamine signaling is observed in other brain areas, and the primary clearance mechanism is not always the DAT (in contrast to striatum), allowing for more volume transmission

effects due to diffusion. For example, in olfactory glomeruli, clearance is objectively slower than in striatum and appears to be mediated primarily via the catechol-O-methyltransferase (COMT)[71, 72]. Midbrain and central amygdala signals are also relatively slower than striatum, making diffusion a more important mechanism of clearance in these brain regions[22, 73]. Interestingly, diffusional impact appears to increase with higher dopamine concentrations, as can be seen in pressure ejection 74 and iontophoresis studies 75. These studies highlight that various mechanisms play a role in clearance. A 2-compartment diffusion model has been used previously and is a highly effective approach for measuring clearance from exogenous catecholamine perfusion[67, 76, 77]. It will be interesting to see how the present unbiased measures contribute to these diffusion based models in the future, as well as how these measures are applied to other neurotransmitters or detection techniques.

In addition to downward velocity, a measure of exponential decay (tau) was also applied to the data. Increasing concentrations of DAT blockers resulted in higher values of tau *ex vivo*. These higher values of tau corresponded with the relative potency of the DAT blocker (highest for WF23 and lowest for cocaine). Similarly, *in vivo* experiments revealed a large increase of tau for mice with WF23 injections and a much smaller increase for mice with PTT injections. This corresponds to the Michaelis-Menten K_m, which increases with lower enzymatic affinity for a substrate 5. Thus, the present study asserts the use of both downward velocity and tau as complementary ways to analyze DAT kinetics independent of the Michaelis-Menten model. We anticipate that the use of the unbiased measures of velocity and exponential decay will be favored by others for their ease of use and reduced user input. We expect that the use of these measures as a complement to Michaelis-Menten approaches may help reduce experimenter error. Lastly, the use of this approach allows for interpretations outside of Michaelis-Menten based assumptions, for instance in brain regions where the DAT is not the predominate mode of clearance. This last application will facilitate our understanding our neurotransmitter dynamics and how these are affected in drug and disease states.

Materials & Methods

Animals

Male and Female (Jackson Laboratory, Sacramento, CA) WT and DATKO (~25–35 g) mice on C57Bl/6 background were given ad libitum access to food and water and maintained on a 12:12-h light/dark cycle. All protocols and animal care procedures were in accordance with the National Institutes of Health Guide for the Care and Use of Laboratory Animals and approved by Brigham Young University Institutional Animal Care and Use Committee, Oregon Health and Science, Drexel University College of Medicine, and Wake Forest University Health Sciences.

Brain Slice Preparation and Drug Application

Isoflurane (Patterson Veterinary, Devens, MA) anesthetized mice were sacrificed by decapitation and brains were rapidly removed, sectioned into thick coronal striatal slices (300–400μm; Leica VT1000S, Vashaw Scientific, Norcross, GA), incubated for 60 minutes at 34 °C in pre-oxygenated (95% O2/5% CO2) artificial cerebral spinal fluid (aCSF).

The aCSF consisted of (in mM): NaCl (126), KCl (2.5), NaH2PO4 (1.2), MgCl2 (1.2), NaHCO3 (25), D-glucose (11), L-ascorbic acid (0.4), with pH adjusted to ~7.4. Cutting solution also contained either MK801 (10 μM; (5S,10R)-(+)-5-methyl-10,11-dihydro-5H-dibenzo[a,d]cyclohepten-5,10-imine; Abcam, Cambridge, UK) or kynurenic acid (2 mM) for blockade of ionotropic glutamate receptors. At the end of the incubation period, tissue was transferred to aCSF (34 °C) without glutamate receptor blockers. The following concentrations of drugs were bath applied for slice voltammetry experiments where specified: Baclofen (30 μM), CGP55845 (200 nM), quinpirole (10 μM), sulpiride (600 nM; Sigma), 2β-propanoyl-3β-(2-naphthyl)-tropane (WF-23) (10 nM – 3 μM; Huw M. L. Davies, Emory University, Atlanta DA), 2β-propanoyl-3β -(4-tolyl)-tropane (PTT) (100 nM – 30 μM; Huw M. L. Davies), cocaine (300 nM - 30 μM; NIDA, Rockville, MD USA).

Ex Vivo Voltammetry Recordings

Slices were transferred to the recording chamber, and perfused with aCSF (34 °C) at a rate of ~1.8 ml/min. Fast scan cyclic voltammetry recordings were performed and analyzed using Demon Voltammetry and Analysis software 6. Carbon fiber electrodes used in voltammetry experiments were made in-house. The carbon fiber (7 μm diameter, Thornel T-650, Cytec, Woodland Park, NJ) was aspirated into a borosilicate glass capillary tube (TW150, World Precision Instruments, Sarasota, FL). Electrodes were then pulled using a pipette puller and cut so that 100–150 μm of carbon fiber protruded from the tip of the glass. The electrode potential was linearly scanned as a triangular waveform from −0.4 to 1.2 V and back to −0.4 V (Ag vs AgCl) with a scan rate of 400 V/sec, repeated every 100 ms. Carbon fiber electrodes were positioned ~250 μm below the slice surface. For baclofen and quinpirole experiments, dopamine release was evoked through electrical stimulation (1 pulse/min) via a glass micropipette (30 μA, 0.5 ms), repeated every 2 minutes. For calcium and DATKO experiments, dopamine release was evoked from a bipolar stimulating electrode (Plastics One, Roanoke, VA) with stimulations at 1 pulse, 5 pulses at 20 Hz, or 24 pulses at 60 Hz (300 μA, 4 msec) applied to the tissue every 5 minutes. Multiple pulse stimulation parameters were selected to model the different *in vivo* firing patterns of dopamine neurons[78, 79]. For baseline collections, stimulations were applied every 2 or 5 minutes until a stable baseline was established (3 collections within 10% variability). Next, either drug or stimulation conditions were changed as noted in the results.

In Vivo Voltammetry Recordings

On the day of testing, mice were anesthetized with urethane (1.5 g/kg, i.p.; Sigma-Aldrich, St. Louis, MO, USA) and implanted with an intravenous (i.v.) catheter as previously described[80, 81]. All drugs for *in vivo* experiments were dissolved in 0.9% saline. Mice were subsequently placed in a stereotaxic apparatus while a stimulating electrode was lowered into the ventral tegmental area (VTA) (-3.0 A/P, +1.0 M/L, −4.5 – 5.0 D/V), a carbon fiber electrode was lowered into the dorsal caudate (+1.3 A/P, +1.3 M/L, −3.0 D/V) and a reference electrode was implanted in the contralateral cortex (+1.5 A/P, −1.5 M/L, −2.0 D/V) 81. Dopamine release was elicited via electrical stimulation of the VTA using 0.4 – 1 sec, 60 Hz monophasic (24p, 4 ms; ~400 μA) stimulation trains. The length of stimulation was varied to ensure sufficient dopamine release across experiments. Baseline dopamine response parameters were collected in 5-minute intervals for a minimum of 30 minutes

prior to drug injection. Once a stable baseline of three consecutive collections was obtained (defined as dopamine peak height within 15%), mice received a single ~200 μL i.v. (2 sec) injection of WF-23 (5.0 mg/kg n = 7), PTT (5.0 mg/kg n = 7) or cocaine (1.5 mg/kg n=6). Evoked dopamine release was measured at 30- and 60-seconds post injection and every 5 minutes thereafter until a peak drug effect was established.

Data Analysis and Statistics

The magnitude of electrically-evoked dopamine release (peak height) and transporter-mediated uptake were monitored and dopamine overflow curves were fitted to an exponential decay model and expressed as tau (time to ~33% of peak height; units in seconds). Data were also modeled using the Michaelis-Menten fit or using the fastest upward or downward velocity calculated from the first derivative of the release trace. All data were analyzed using Demon Voltammetry and Analysis software 6 written in LabVIEW (National Instruments, Austin, TX).

Carbon fiber electrodes were initially calibrated using low (1 μM) and high (10 μM) dopamine concentrations, which was compared back to background current amplitude for establishing a model based on linear regression for calibration values. The resultant linear regression model was applied to electrodes for determining the relative calibration constant. Statistics were performed using Prism 5 (GraphPad, San Diego, CA) and NCSS 8 (NCSS LLC, Kaysville UT). Statistical significance was determined for groups of 2 variables using a two-tailed student t-test. Experiments with more than 2 groups, but only one factor, were tested for significance using a one-way analysis of variance (ANOVA). Data from multiple time points within the same experiment were analyzed with a repeated measures ANOVA (RM-ANOVA). For experiments that examined multiple factors and interactions, two-way ANOVA or RM-ANOVAs were used. Tukey's HSD and Bonferroni correction methods were used for post-ANOVA analysis. For figures where raw traces are shown that are described as having "slow" or "fast" downward velocity (e.g. Figures 4 and 7), no specific threshold was used for labeling a signal as "slow" or "fast"; described velocity is relative to other experiments from the same dataset.

Supplementary Material

Refer to Web version on PubMed Central for supplementary material.

Acknowledgements:

This work is supported by the US National Institute of Health (NIH) grants DA040409 to JTY, R00 DA04510 to CAS, R01031900 to RAE as well as grants from the Brain and Behavior Research Foundation and Alkermes to CAS, and internal mentored research funding from Brigham Young University College of Life Sciences to JTY. We would also like to thank Caylor Hafen, Hillary Wadsworth, Parker Layton for their help in performing blinded Michaelis-Menten analysis. We would also like to thank Jared Willets for assistance in graphic design.

References

1. Ferris MJ, Calipari ES, Yorgason JT, and Jones SR (2013) Examining the complex regulation and drug-induced plasticity of dopamine release and uptake using voltammetry in brain slices, ACS Chem Neurosci 4, 693–703. [PubMed: 23581570]

2. Li Y, and Ross AE (2020) Plasma-treated carbon-fiber microelectrodes for improved purine detection with fast-scan cyclic voltammetry, Analyst 145, 805–815. [PubMed: 31820742]
3. Spanos M, Gras-Najjar J, Letchworth JM, Sanford AL, Toups JV, and Sombers LA (2013) Quantitation of hydrogen peroxide fluctuations and their modulation of dopamine dynamics in the rat dorsal striatum using fast-scan cyclic voltammetry, ACS Chem Neurosci 4, 782–789. [PubMed: 23556461]
4. Wightman RM (1988) Voltammetry with microscopic electrodes in new domains, Science 240, 415–420. [PubMed: 17784064]
5. Wightman RM, and Zimmerman JB (1990) Control of dopamine extracellular concentration in rat striatum by impulse flow and uptake, Brain Res Brain Res Rev 15, 135–144. [PubMed: 2282449]
6. Yorgason JT, Espana RA, and Jones SR (2011) Demon voltammetry and analysis software: analysis of cocaine-induced alterations in dopamine signaling using multiple kinetic measures, J Neurosci Methods 202, 158–164. [PubMed: 21392532]
7. Wu Q, Reith ME, Kuhar MJ, Carroll FI, and Garris PA (2001) Preferential increases in nucleus accumbens dopamine after systemic cocaine administration are caused by unique characteristics of dopamine neurotransmission, J Neurosci 21, 6338–6347. [PubMed: 11487657]
8. Michaelis L, Menten ML, Johnson KA, and Goody RS (2011) The original Michaelis constant: translation of the 1913 Michaelis-Menten paper, Biochemistry 50, 8264–8269. [PubMed: 21888353]
9. Lopachev A, Volnova A, Evdokimenko A, Abaimov D, Timoshina Y, Kazanskaya R, Lopacheva O, Deal A, Budygin E, Fedorova T, and Gainetdinov R (2019) Intracerebroventricular injection of ouabain causes mania-like behavior in mice through D2 receptor activation, Sci Rep 9, 15627. [PubMed: 31666560]
10. Pattison LP, McIntosh S, Budygin EA, and Hemby SE (2012) Differential regulation of accumbal dopamine transmission in rats following cocaine, heroin and speedball self-administration, J Neurochem 122, 138–146. [PubMed: 22443145]
11. John CE, and Jones SR (2007) Voltammetric characterization of the effect of monoamine uptake inhibitors and releasers on dopamine and serotonin uptake in mouse caudate-putamen and substantia nigra slices, Neuropharmacology 52, 1596–1605. [PubMed: 17459426]
12. Xiao N, Privman E, and Venton BJ (2014) Optogenetic control of serotonin and dopamine release in Drosophila larvae, ACS Chem Neurosci 5, 666–673. [PubMed: 24849718]
13. Near JA, Bigelow JC, and Wightman RM (1988) Comparison of uptake of dopamine in rat striatal chopped tissue and synaptosomes, J Pharmacol Exp Ther 245, 921–927. [PubMed: 3385647]
14. Torres DJ, Yorgason JT, Andres MA, and Bellinger FP (2021) Methamphetamine Exposure During Development Causes Lasting Changes to Mesolimbic Dopamine Signaling in Mice, Cell Mol Neurobiol.
15. Yorgason JT, Espana RA, Konstantopoulos JK, Weiner JL, and Jones SR (2013) Enduring increases in anxiety-like behavior and rapid nucleus accumbens dopamine signaling in socially isolated rats, Eur J Neurosci 37, 1022–1031. [PubMed: 23294165]
16. Calipari ES, Ferris MJ, Siciliano CA, and Jones SR (2015) Differential influence of dopamine transport rate on the potencies of cocaine, amphetamine, and methylphenidate, ACS Chem Neurosci 6, 155–162. [PubMed: 25474655]
17. Ramsson ES, Covey DP, Daberkow DP, Litherland MT, Juliano SA, and Garris PA (2011) Amphetamine augments action potential-dependent dopaminergic signaling in the striatum in vivo, J Neurochem 117, 937–948. [PubMed: 21443523]
18. Siciliano CA, Mauterer MI, Fordahl SC, and Jones SR (2019) Modulation of striatal dopamine dynamics by cocaine self-administration and amphetamine treatment in female rats, Eur J Neurosci 50, 2740–2749. [PubMed: 31111573]
19. Yorgason JT, Calipari ES, Ferris MJ, Karkhanis AN, Fordahl SC, Weiner JL, and Jones SR (2016) Social isolation rearing increases dopamine uptake and psychostimulant potency in the striatum, Neuropharmacology 101, 471–479. [PubMed: 26525189]
20. Torres DJ, Yorgason JT, Mitchell CC, Hagiwara A, Andres MA, Kurokawa S, Steffensen SC, and Bellinger FP (2021) Selenoprotein P Modulates Methamphetamine Enhancement of Vesicular

Dopamine Release in Mouse Nucleus Accumbens Via Dopamine D2 Receptors, Front Neurosci 15, 631825. [PubMed: 33927588]

21. Yorgason JT, Ferris MJ, Steffensen SC, and Jones SR (2014) Frequency-dependent effects of ethanol on dopamine release in the nucleus accumbens, Alcohol Clin Exp Res 38, 438–447. [PubMed: 24117706]
22. Ford CP, Gantz SC, Phillips PE, and Williams JT (2010) Control of extracellular dopamine at dendrite and axon terminals, J Neurosci 30, 6975–6983. [PubMed: 20484639]
23. Karkhanis AN, Leach AC, Yorgason JT, Uneri A, Barth S, Niere F, Alexander NJ, Weiner JL, McCool BA, Raab-Graham KF, Ferris MJ, and Jones SR (2019) Chronic Social Isolation Stress during Peri-Adolescence Alters Presynaptic Dopamine Terminal Dynamics via Augmentation in Accumbal Dopamine Availability, ACS Chem Neurosci 10, 2033–2044. [PubMed: 30284806]
24. Bisgaard H, Larsen MA, Mazier S, Beuming T, Newman AH, Weinstein H, Shi L, Loland CJ, and Gether U (2011) The binding sites for benztropines and dopamine in the dopamine transporter overlap, Neuropharmacology 60, 182–190. [PubMed: 20816875]
25. Beuming T, Kniazeff J, Bergmann ML, Shi L, Gracia L, Raniszewska K, Newman AH, Javitch JA, Weinstein H, Gether U, and Loland CJ (2008) The binding sites for cocaine and dopamine in the dopamine transporter overlap, Nat Neurosci 11, 780–789. [PubMed: 18568020]
26. Wang KH, Penmatsa A, and Gouaux E (2015) Neurotransmitter and psychostimulant recognition by the dopamine transporter, Nature 521, 322–327. [PubMed: 25970245]
27. Davies HM, Saikali E, Huby NJ, Gilliatt VJ, Matasi JJ, Sexton T, and Childers SR (1994) Synthesis of 2 beta-acyl-3 beta-aryl-8-azabicyclo[3.2.1]octanes and their binding affinities at dopamine and serotonin transport sites in rat striatum and frontal cortex, J Med Chem 37, 1262–1268. [PubMed: 8176704]
28. Bennett BA, Wichems CH, Hollingsworth CK, Davies HM, Thornley C, Sexton T, and Childers SR (1995) Novel 2-substituted cocaine analogs: uptake and ligand binding studies at dopamine, serotonin and norepinephrine transport sites in the rat brain, J Pharmacol Exp Ther 272, 1176–1186. [PubMed: 7891330]
29. Letchworth SR, Smith HR, Porrino LJ, Bennett BA, Davies HM, Sexton T, and Childers SR (2000) Characterization of a tropane radioligand, [(3)H]2beta-propanoyl-3beta-(4-tolyl) tropane ([(3)H]PTT), for dopamine transport sites in rat brain, J Pharmacol Exp Ther 293, 686–696. [PubMed: 10773045]
30. Gatley SJ, Pan D, Chen R, Chaturvedi G, and Ding YS (1996) Affinities of methylphenidate derivatives for dopamine, norepinephrine and serotonin transporters, Life Sci 58, 231–239. [PubMed: 8786705]
31. Katz JL, Izenwasser S, and Terry P (2000) Relationships among dopamine transporter affinities and cocaine-like discriminative-stimulus effects, Psychopharmacology (Berl) 148, 90–98. [PubMed: 10663422]
32. Calipari ES, Ferris MJ, Siciliano CA, Zimmer BA, and Jones SR (2014) Intermittent cocaine self-administration produces sensitization of stimulant effects at the dopamine transporter, J Pharmacol Exp Ther 349, 192–198. [PubMed: 24566123]
33. Siciliano CA, Calipari ES, Ferris MJ, and Jones SR (2015) Adaptations of presynaptic dopamine terminals induced by psychostimulant self-administration, ACS Chem Neurosci 6, 27–36. [PubMed: 25491345]
34. Jones SR, Gainetdinov RR, Wightman RM, and Caron MG (1998) Mechanisms of amphetamine action revealed in mice lacking the dopamine transporter, J Neurosci 18, 1979–1986. [PubMed: 9482784]
35. Benoit-Marand M, Jaber M, and Gonon F (2000) Release and elimination of dopamine in vivo in mice lacking the dopamine transporter: functional consequences, Eur J Neurosci 12, 2985–2992. [PubMed: 10971639]
36. Gasser PJ (2019) Roles for the uptake2 transporter OCT3 in regulation of dopaminergic neurotransmission and behavior, Neurochem Int 123, 46–49. [PubMed: 30055194]
37. Kimmel HL, Joyce AR, Carroll FI, and Kuhar MJ (2001) Dopamine D1 and D2 receptors influence dopamine transporter synthesis and degradation in the rat, J Pharmacol Exp Ther 298, 129–140. [PubMed: 11408534]

38. Pillai G, Brown NA, McAllister G, Milligan G, and Seabrook GR (1998) Human D2 and D4 dopamine receptors couple through betagamma G-protein subunits to inwardly rectifying K+ channels (GIRK1) in a Xenopus oocyte expression system: selective antagonism by L-741,626 and L-745,870 respectively, Neuropharmacology 37, 983–987. [PubMed: 9833627]
39. Greco PG, and Garris PA (2003) In vivo interaction of cocaine with the dopamine transporter as measured by voltammetry, Eur J Pharmacol 479, 117–125. [PubMed: 14612143]
40. Einhorn LC, Johansen PA, and White FJ (1988) Electrophysiological effects of cocaine in the mesoaccumbens dopamine system: studies in the ventral tegmental area, J Neurosci 8, 100–112. [PubMed: 3339402]
41. Phillips PE, Hancock PJ, and Stamford JA (2002) Time window of autoreceptor-mediated inhibition of limbic and striatal dopamine release, Synapse 44, 15–22. [PubMed: 11842442]
42. Kennedy RT, Jones SR, and Wightman RM (1992) Dynamic observation of dopamine autoreceptor effects in rat striatal slices, J Neurochem 59, 449–455. [PubMed: 1352798]
43. Burrell MH, Atcherley CW, Heien ML, and Lipski J (2015) A novel electrochemical approach for prolonged measurement of absolute levels of extracellular dopamine in brain slices, ACS Chem Neurosci 6, 1802–1812. [PubMed: 26322962]
44. Yee AG, Forbes B, Cheung PY, Martini A, Burrell MH, Freestone PS, and Lipski J (2019) Action potential and calcium dependence of tonic somatodendritic dopamine release in the Substantia Nigra pars compacta, J Neurochem 148, 462–479. [PubMed: 30203851]
45. Marcott PF, Mamaligas AA, and Ford CP (2014) Phasic dopamine release drives rapid activation of striatal D2-receptors, Neuron 84, 164–176. [PubMed: 25242218]
46. Holroyd KB, Adrover MF, Fuino RL, Bock R, Kaplan AR, Gremel CM, Rubinstein M, and Alvarez VA (2015) Loss of feedback inhibition via D2 autoreceptors enhances acquisition of cocaine taking and reactivity to drug-paired cues, Neuropsychopharmacology 40, 1495–1509. [PubMed: 25547712]
47. Adrover MF, Shin JH, and Alvarez VA (2014) Glutamate and dopamine transmission from midbrain dopamine neurons share similar release properties but are differentially affected by cocaine, J Neurosci 34, 3183–3192. [PubMed: 24573277]
48. Yorgason JT, Zeppenfeld DM, and Williams JT (2017) Cholinergic Interneurons Underlie Spontaneous Dopamine Release in Nucleus Accumbens, J Neurosci 37, 2086–2096. [PubMed: 28115487]
49. Ferraro L, Beggiato S, Marcellino D, Frankowska M, Filip M, Agnati LF, Antonelli T, Tomasini MC, Tanganelli S, and Fuxe K (2010) Nanomolar concentrations of cocaine enhance D2-like agonist-induced inhibition of the K+-evoked [3H]-dopamine efflux from rat striatal synaptosomes: a novel action of cocaine, J Neural Transm (Vienna) 117, 593–597. [PubMed: 20354886]
50. Genedani S, Carone C, Guidolin D, Filaferro M, Marcellino D, Fuxe K, and Agnati LF (2010) Differential sensitivity of A2A and especially D2 receptor trafficking to cocaine compared with lipid rafts in cotransfected CHO cell lines. Novel actions of cocaine independent of the DA transporter, J Mol Neurosci 41, 347–357. [PubMed: 20143275]
51. Ferraro L, Frankowska M, Marcellino D, Zaniewska M, Beggiato S, Filip M, Tomasini MC, Antonelli T, Tanganelli S, and Fuxe K (2012) A novel mechanism of cocaine to enhance dopamine d2-like receptor mediated neurochemical and behavioral effects. An in vivo and in vitro study, Neuropsychopharmacology 37, 1856–1866. [PubMed: 22453136]
52. Fulton S, Thibault D, Mendez JA, Lahaie N, Tirotta E, Borrelli E, Bouvier M, Tempel BL, and Trudeau LE (2011) Contribution of Kv1.2 voltage-gated potassium channel to D2 autoreceptor regulation of axonal dopamine overflow, J Biol Chem 286, 9360–9372. [PubMed: 21233214]
53. Blackmer T, Larsen EC, Takahashi M, Martin TF, Alford S, and Hamm HE (2001) G protein betagamma subunit-mediated presynaptic inhibition: regulation of exocytotic fusion downstream of Ca2+ entry, Science 292, 293–297. [PubMed: 11303105]
54. Chen R, Ferris MJ, and Wang S (2020) Dopamine D2 autoreceptor interactome: Targeting the receptor complex as a strategy for treatment of substance use disorder, Pharmacol Ther 213, 107583. [PubMed: 32473160]

55. Guatteo E, Bengtson CP, Bernardi G, and Mercuri NB (2004) Voltage-gated calcium channels mediate intracellular calcium increase in weaver dopaminergic neurons during stimulation of D2 and GABAB receptors, J Neurophysiol 92, 3368–3374. [PubMed: 15240766]
56. Wang L, Zhang X, Xu H, Zhou L, Jiao R, Liu W, Zhu F, Kang X, Liu B, Teng S, Wu Q, Li M, Dou H, Zuo P, Wang C, Wang S, and Zhou Z (2014) Temporal components of cholinergic terminal to dopaminergic terminal transmission in dorsal striatum slices of mice, J Physiol 592, 3559–3576. [PubMed: 24973407]
57. Gao F, Chen D, Ma X, Sudweeks S, Yorgason JT, Gao M, Turner D, Eaton JB, McIntosh JM, Lukas RJ, Whiteaker P, Chang Y, Steffensen SC, and Wu J (2019) Alpha6-containing nicotinic acetylcholine receptor is a highly sensitive target of alcohol, Neuropharmacology 149, 45–54. [PubMed: 30710570]
58. Brimblecombe KR, Gracie CJ, Platt NJ, and Cragg SJ (2015) Gating of dopamine transmission by calcium and axonal N-, Q-, T- and L-type voltage-gated calcium channels differs between striatal domains, J Physiol 593, 929–946. [PubMed: 25533038]
59. Chen YA, Scales SJ, Patel SM, Doung YC, and Scheller RH (1999) SNARE complex formation is triggered by Ca2+ and drives membrane fusion, Cell 97, 165–174. [PubMed: 10219238]
60. Acevedo-Rodriguez A, Zhang L, Zhou F, Gong S, Gu H, De Biasi M, Zhou FM, and Dani JA (2014) Cocaine inhibition of nicotinic acetylcholine receptors influences dopamine release, Front Synaptic Neurosci 6, 19. [PubMed: 25237305]
61. Wheeler DS, Ebben AL, Kurtoglu B, Lovell ME, Bohn AT, Jasek IA, Baker DA, Mantsch JR, Gasser PJ, and Wheeler RA (2017) Corticosterone regulates both naturally occurring and cocaine-induced dopamine signaling by selectively decreasing dopamine uptake, Eur J Neurosci 46, 2638–2646. [PubMed: 28965353]
62. Holleran KM, Rose JH, Fordahl SC, Benton KC, Rohr KE, Gasser PJ, and Jones SR (2020) Organic cation transporter 3 and the dopamine transporter differentially regulate catecholamine uptake in the basolateral amygdala and nucleus accumbens, Eur J Neurosci 52, 4546–4562. [PubMed: 32725894]
63. Lloyd JT, Yee AG, Kalligappa PK, Jabed A, Cheung PY, Todd KL, Karunasinghe RN, Vlajkovic SM, Freestone PS, and Lipski J (2022) Dopamine Dysregulation and Altered Responses to Drugs Affecting Dopaminergic Transmission in a New Dopamine Transporter Knockout (DAT-KO) Rat Model, Neuroscience.
64. Kile BM, Guillot TS, Venton BJ, Wetsel WC, Augustine GJ, and Wightman RM (2010) Synapsins differentially control dopamine and serotonin release, J Neurosci 30, 9762–9770. [PubMed: 20660258]
65. Courtney NA, and Ford CP (2014) The timing of dopamine- and noradrenaline-mediated transmission reflects underlying differences in the extent of spillover and pooling, J Neurosci 34, 7645–7656. [PubMed: 24872568]
66. Ford CP, Phillips PE, and Williams JT (2009) The time course of dopamine transmission in the ventral tegmental area, J Neurosci 29, 13344–13352. [PubMed: 19846722]
67. Sykova E, and Nicholson C (2008) Diffusion in brain extracellular space, Physiol Rev 88, 1277–1340. [PubMed: 18923183]
68. Giros B, Jaber M, Jones SR, Wightman RM, and Caron MG (1996) Hyperlocomotion and indifference to cocaine and amphetamine in mice lacking the dopamine transporter, Nature 379, 606–612. [PubMed: 8628395]
69. Jones SR, Gainetdinov RR, Jaber M, Giros B, Wightman RM, and Caron MG (1998) Profound neuronal plasticity in response to inactivation of the dopamine transporter, Proc Natl Acad Sci U S A 95, 4029–4034. [PubMed: 9520487]
70. Leo D, Sukhanov I, Zoratto F, Illiano P, Caffino L, Sanna F, Messa G, Emanuele M, Esposito A, Dorofeikova M, Budygin EA, Mus L, Efimova EV, Niello M, Espinoza S, Sotnikova TD, Hoener MC, Laviola G, Fumagalli F, Adriani W, and Gainetdinov RR (2018) Pronounced Hyperactivity, Cognitive Dysfunctions, and BDNF Dysregulation in Dopamine Transporter Knock-out Rats, J Neurosci 38, 1959–1972. [PubMed: 29348190]

71. Vaaga CE, Yorgason JT, Williams JT, and Westbrook GL (2017) Presynaptic gain control by endogenous cotransmission of dopamine and GABA in the olfactory bulb, J Neurophysiol 117, 1163–1170. [PubMed: 28031402]

72. Cockerham R, Liu S, Cachope R, Kiyokage E, Cheer JF, Shipley MT, and Puche AC (2016) Subsecond Regulation of Synaptically Released Dopamine by COMT in the Olfactory Bulb, J Neurosci 36, 7779–7785. [PubMed: 27445153]

73. Hedges DM, Yorgason JT, Brundage JN, Wadsworth HA, Williams B, Steffensen SC, and Roberto M (2020) Corticotropin releasing factor, but not alcohol, modulates norepinephrine release in the rat central nucleus of the amygdala, Neuropharmacology 179, 108293. [PubMed: 32871155]

74. Vickrey TL, Xiao N, and Venton BJ (2013) Kinetics of the dopamine transporter in Drosophila larva, ACS Chem Neurosci 4, 832–837. [PubMed: 23600464]

75. Nicholson C (1995) Interaction between diffusion and Michaelis-Menten uptake of dopamine after iontophoresis in striatum, Biophys J 68, 1699–1715. [PubMed: 7612814]

76. Walters SH, Taylor IM, Shu Z, and Michael AC (2014) A novel restricted diffusion model of evoked dopamine, ACS Chem Neurosci 5, 776–783. [PubMed: 24983330]

77. Hoffman AF, Spivak CE, and Lupica CR (2016) Enhanced Dopamine Release by Dopamine Transport Inhibitors Described by a Restricted Diffusion Model and Fast-Scan Cyclic Voltammetry, ACS Chem Neurosci 7, 700–709. [PubMed: 27018734]

78. Daberkow DP, Brown HD, Bunner KD, Kraniotis SA, Doellman MA, Ragozzino ME, Garris PA, and Roitman MF (2013) Amphetamine paradoxically augments exocytotic dopamine release and phasic dopamine signals, J Neurosci 33, 452–463. [PubMed: 23303926]

79. Zhang L, Doyon WM, Clark JJ, Phillips PE, and Dani JA (2009) Controls of tonic and phasic dopamine transmission in the dorsal and ventral striatum, Mol Pharmacol 76, 396–404. [PubMed: 19460877]

80. Yorgason JT, Jones SR, and Espana RA (2011) Low and high affinity dopamine transporter inhibitors block dopamine uptake within 5 sec of intravenous injection, Neuroscience 182, 125–132. [PubMed: 21402130]

81. Shaw JK, Ferris MJ, Locke JL, Brodnik ZD, Jones SR, and Espana RA (2017) Hypocretin/orexin knock-out mice display disrupted behavioral and dopamine responses to cocaine, Addict Biol 22, 1695–1705. [PubMed: 27480648]

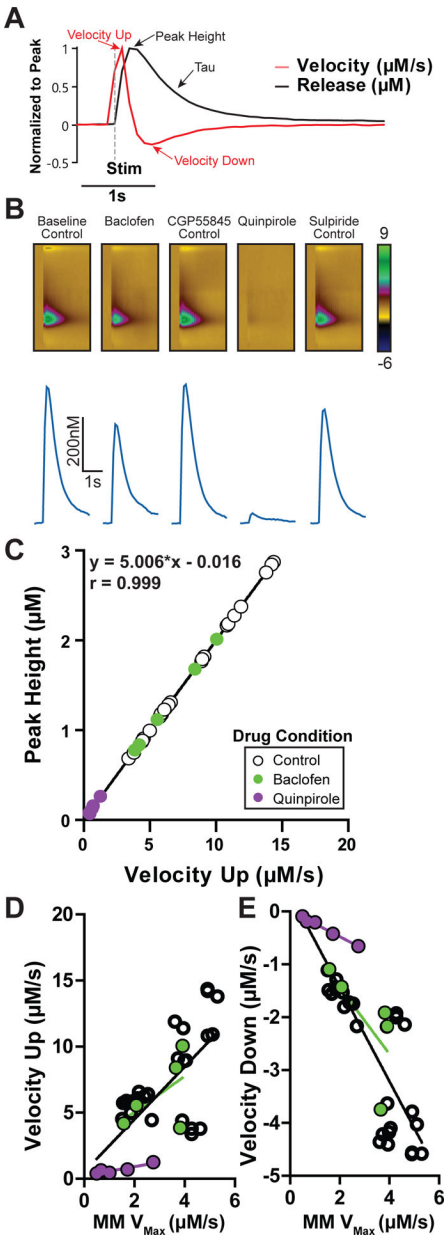

Figure 1. Peak height and upward velocity are related measures of dopamine release and are reduced with D_2 and $GABA_B$ agonists

A) An example dopamine trace is shown under baseline conditions (black), alongside its corresponding first derivative (red; velocity), normalized by peak to highlight how these measures correspond to each other. Time of stimulation (1p, 30 μA) is denoted (gray dashed line). B) Dopamine release is reduced by $GABA_B$ agonist baclofen (30 μM), which is reversed by the $GABA_B$ antagonist CGP55845 (200 nM), which acts as a control for baclofen effects. The D_2 agonist quinpirole (1 μM) robustly inhibits dopamine release, which is reversed by the D_2 antagonist sulpiride (600 nM), which was also treated as a control condition. C) Dopamine release peak height correlates with maximal upward velocity, which is decreased from control conditions during $GABA_B$ and D_2 stimulation.

D) Maximal upward and E) maximal downward velocity significantly correlate to the Michaelis-Menten (MM) V_{max} values across all drug conditions.

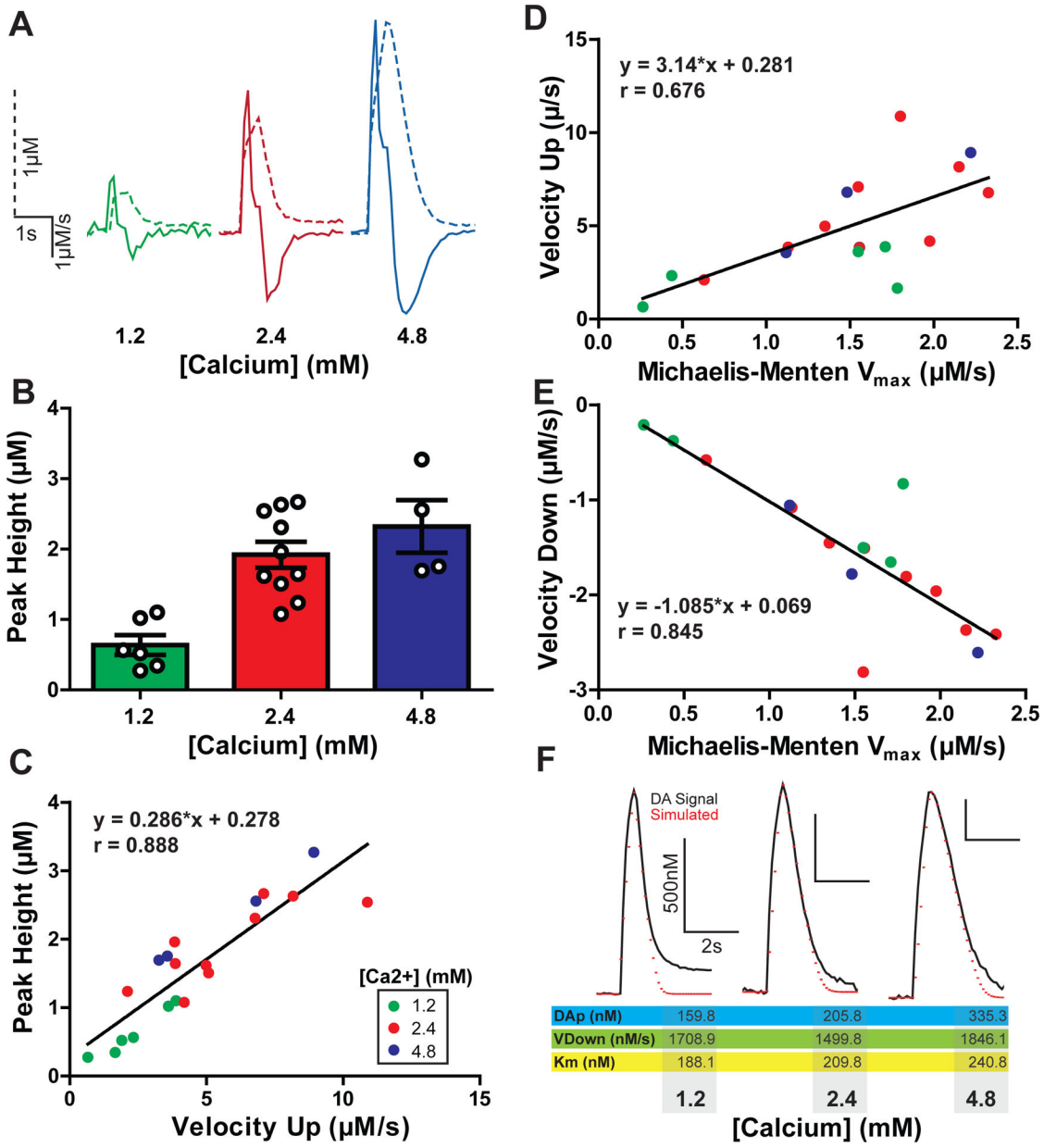

Figure 2. Upward velocity and peak height as measures of changes in dopamine release with calcium

A) A comparison of example dopamine traces (dotted lines) overlaid with the corresponding first derivative (solid lines) at increasing concentrations of calcium. All traces are scaled identically. B) Maximal evoked dopamine concentrations (μM) at increasing concentrations of calcium (mM). C) Maximal upward velocity corresponds linearly with an increase in evoked dopamine release. Calcium concentrations for each measure are denoted by color. D) Upward velocity and E) downward velocity correlate with the Michaelis-Menten V_{max} across all calcium conditions.

F) Voltammetry signals were modeled using Michaelis-Menten protocols where the maximal downward velocity was substituted for the Vmax value. Shown are three example traces (black) from each calcium condition overlayed with simulated modeled data (red) from

these experiments. Below the traces are the Michaelis-Menten parameters obtained through modeling with downward velocity as the V_{max}.

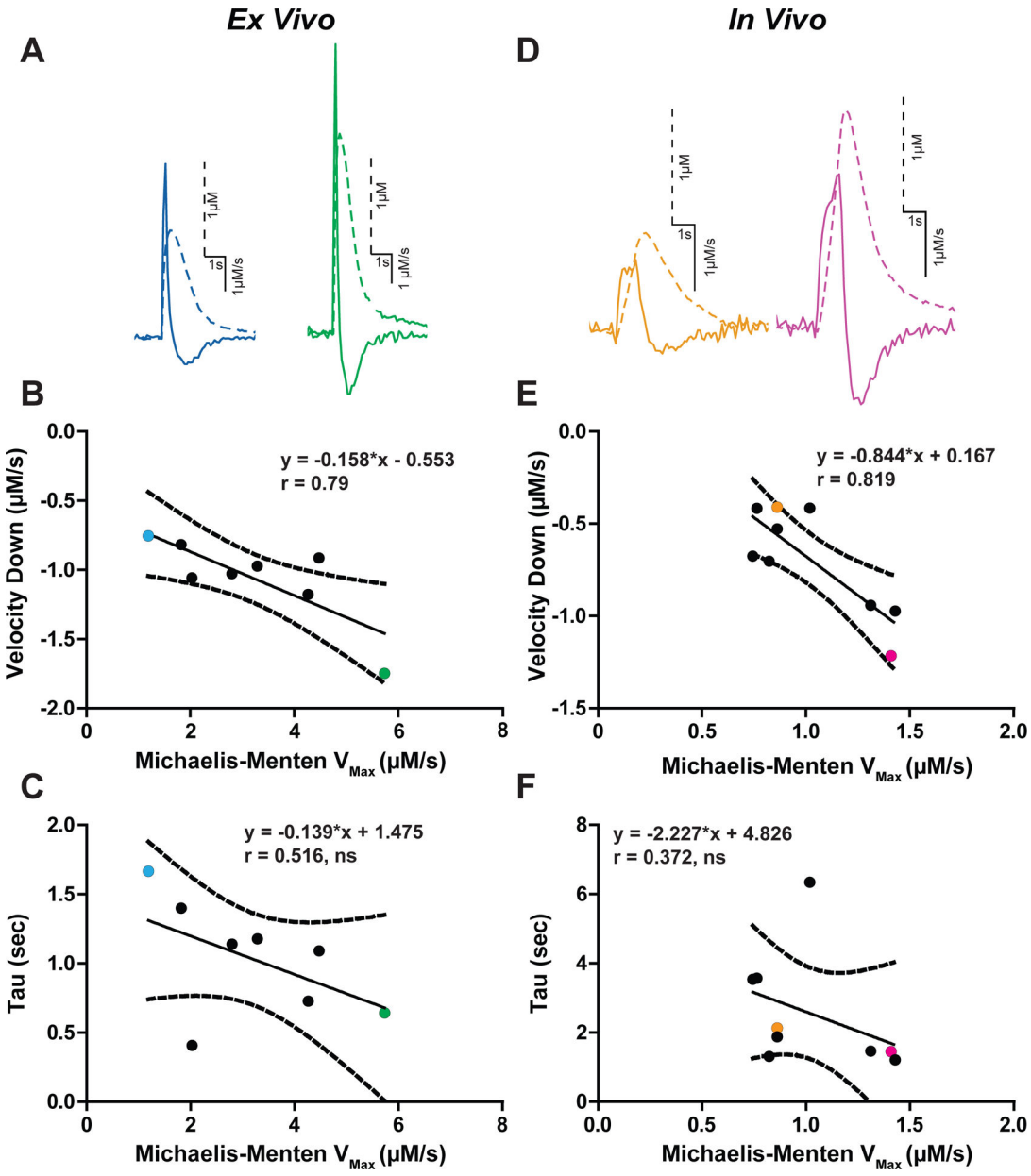

Figure 3. Downward velocity as a measure of dopamine transporter function

Evoked dopamine traces from *ex vivo* (A) and *in vivo* (D) recordings. Traces are scaled individually. Dopamine concentration (dotted lines) and first derivative (solid line) are overlaid. Each trace is scaled individually. B) The V_{max} obtained using the Michaelis-Menten model is plotted against the descending arm of the first derivative (Velocity Down). Each dot represents one experiment from *ex vivo* (B) and *in vivo* (E) experiments, with the colored dots corresponding to their respective colored traces in panels A and D. The exponential decay measure tau was examined against Vmax, and the two measures did not significantly correlate for ex vivo (C) and in vivo (F) experiments. (ns = not significant)

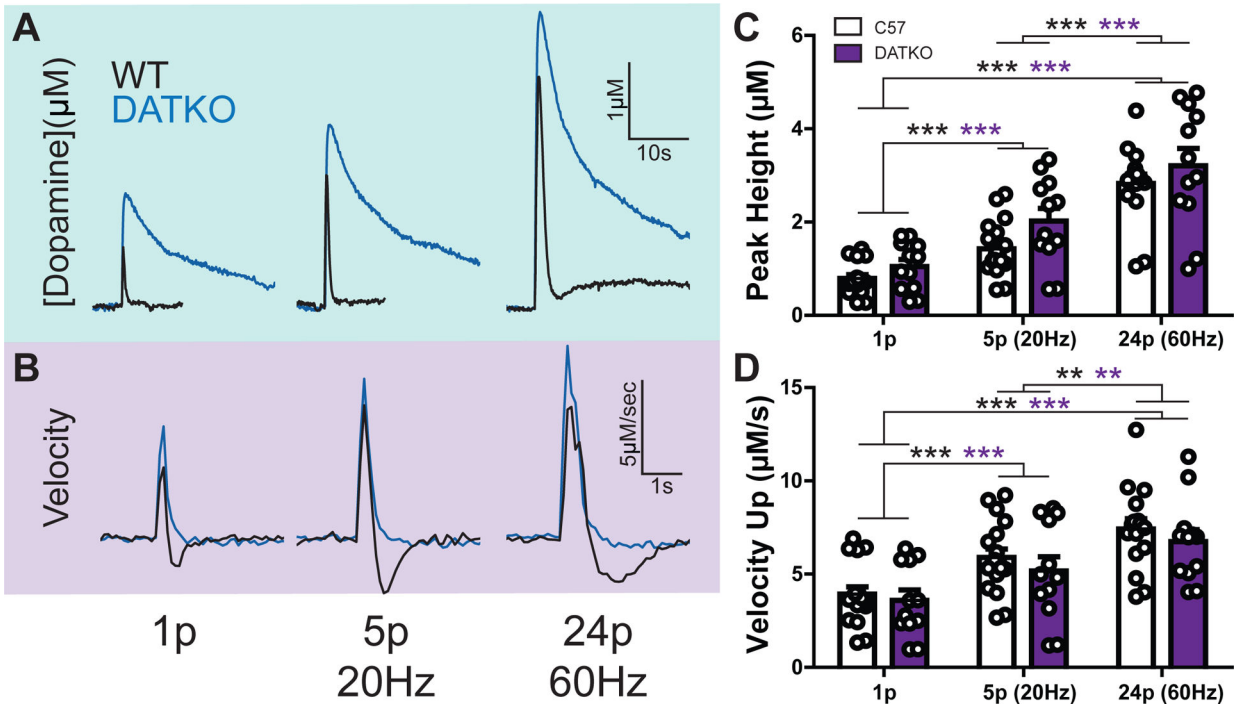

Figure 4. Upward velocity is not indicative of difference in uptake in DAT knockout mice

A) Evoked dopamine release concentrations compared between wild-type (black) and DAT knockout (blue) mice. Increasing pulse number and frequency induced higher release concentrations. Pulse protocols began with a single pulse (left), then increased to 5 pulses at 20 Hz (middle) and ended with 24 pulses at 60 Hz (right). B) The first derivative (velocity) of the dopamine traces in panel A. C) Average peak dopamine concentrations for the three pulse conditions. Each dot represents a single pulse event. D) First derivative maximum (peak velocity) for the three pulse conditions. Each dot represents a single pulse event. (** = $p < 0.01$; *** = $p < 0.001$)

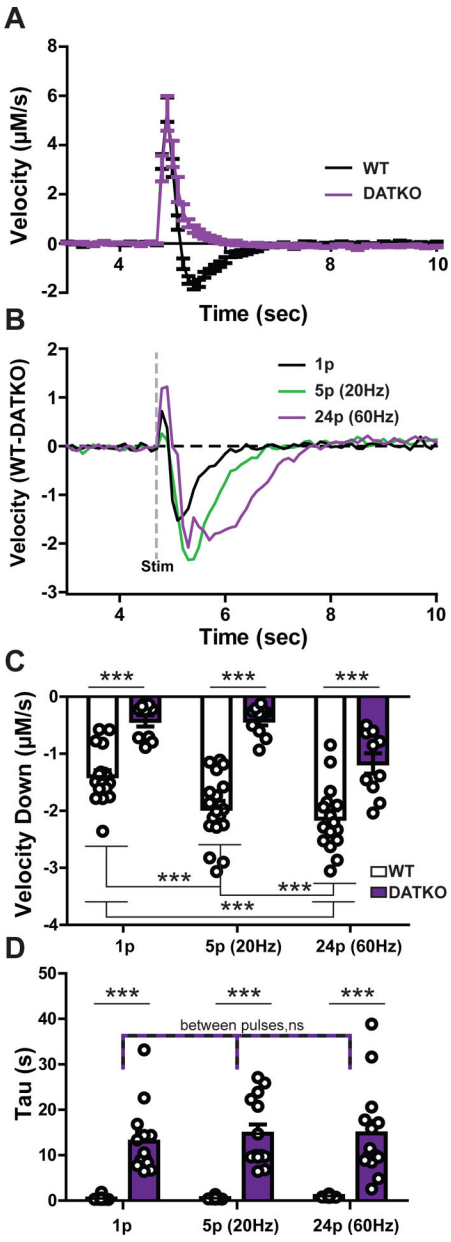

Figure 5. Downward velocity as a measure of dopamine clearance in DAT knockout mice

A) A comparison of wild-type (black line) and DAT knockout (purple line) velocities obtained via the first derivative of dopamine concentration release under the single pulse condition. Note the slow decrease in DATKO compared to the negative values in the WT mouse. B) A subtraction plot of a first derivative trace in a WT mouse minus a trace from the DATKO mouse for each pulse condition. An electrical stimulation was delivered at 5 seconds as denoted by the dashed grey line. C) Average minima for the first derivative (peak velocity down) and D) exponential decay measure tau compared by mouse type and pulse condition. Each dot denotes a single dopamine release event. (*** = $p < 0.001$; ns = not significant)

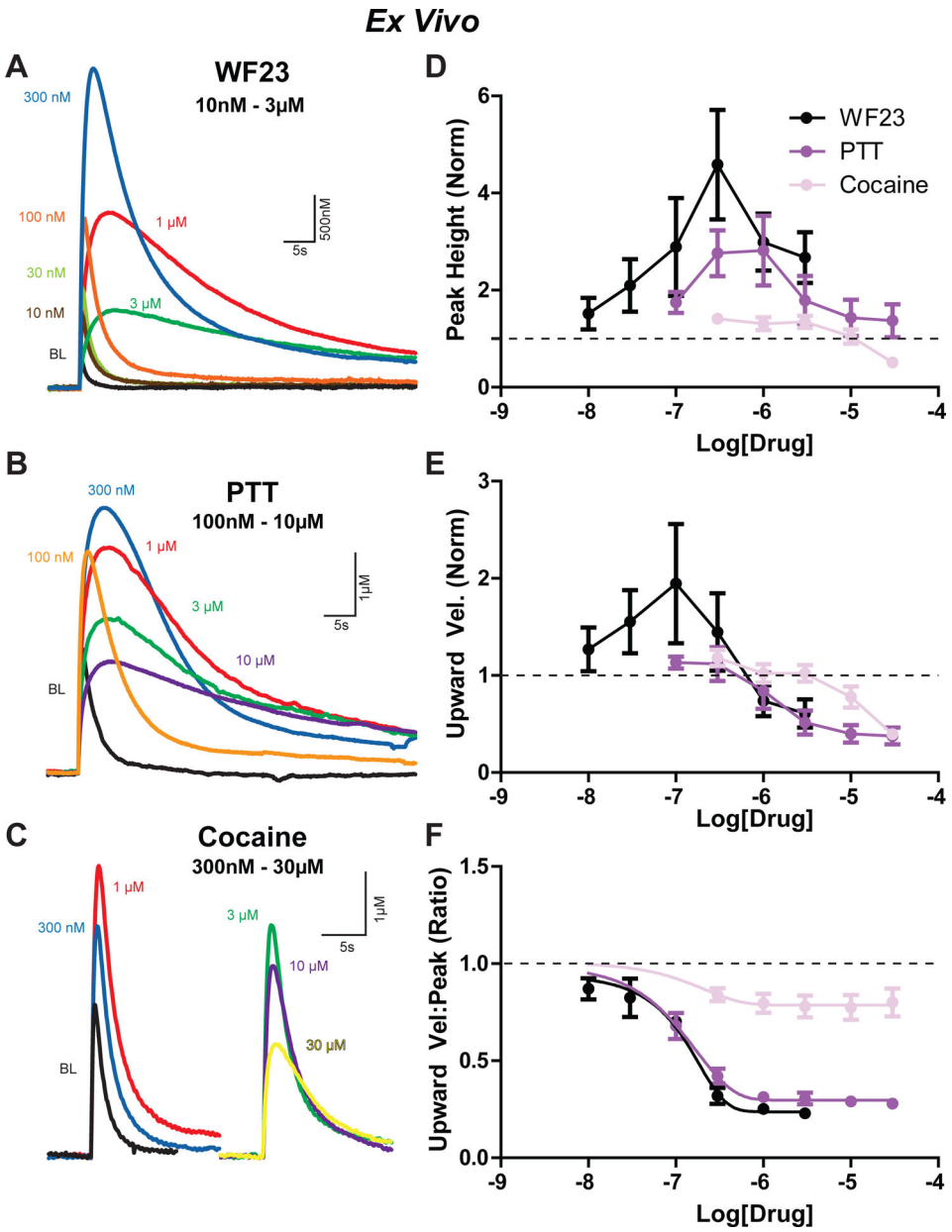

Figure 6. Effects of DAT blockers on dopamine release kinetics ex vivo

Traces from A) WF23 (10 nM – 3 μM), B) PTT (100 nM – 30 μM, and C) cocaine (300 nM – 30 μM) drug concentrations found in Figures 6D, E, and F, respectively. Signals denoted by color: baseline (black), 10 nM (brown), 30 nM (yellow-green), 100 nM (orange), 300 nM (blue), 1 μM (red), 3 μM (green), 30 μM (yellow). D) Comparison of peak height of signals across concentrations for WF23 (black), PTT (purple), and cocaine (pink). Similar comparisons across drug concentrations for E) upwards velocity and F) the ratio of upwards velocity to peak height. All measurements are normalized to baseline.

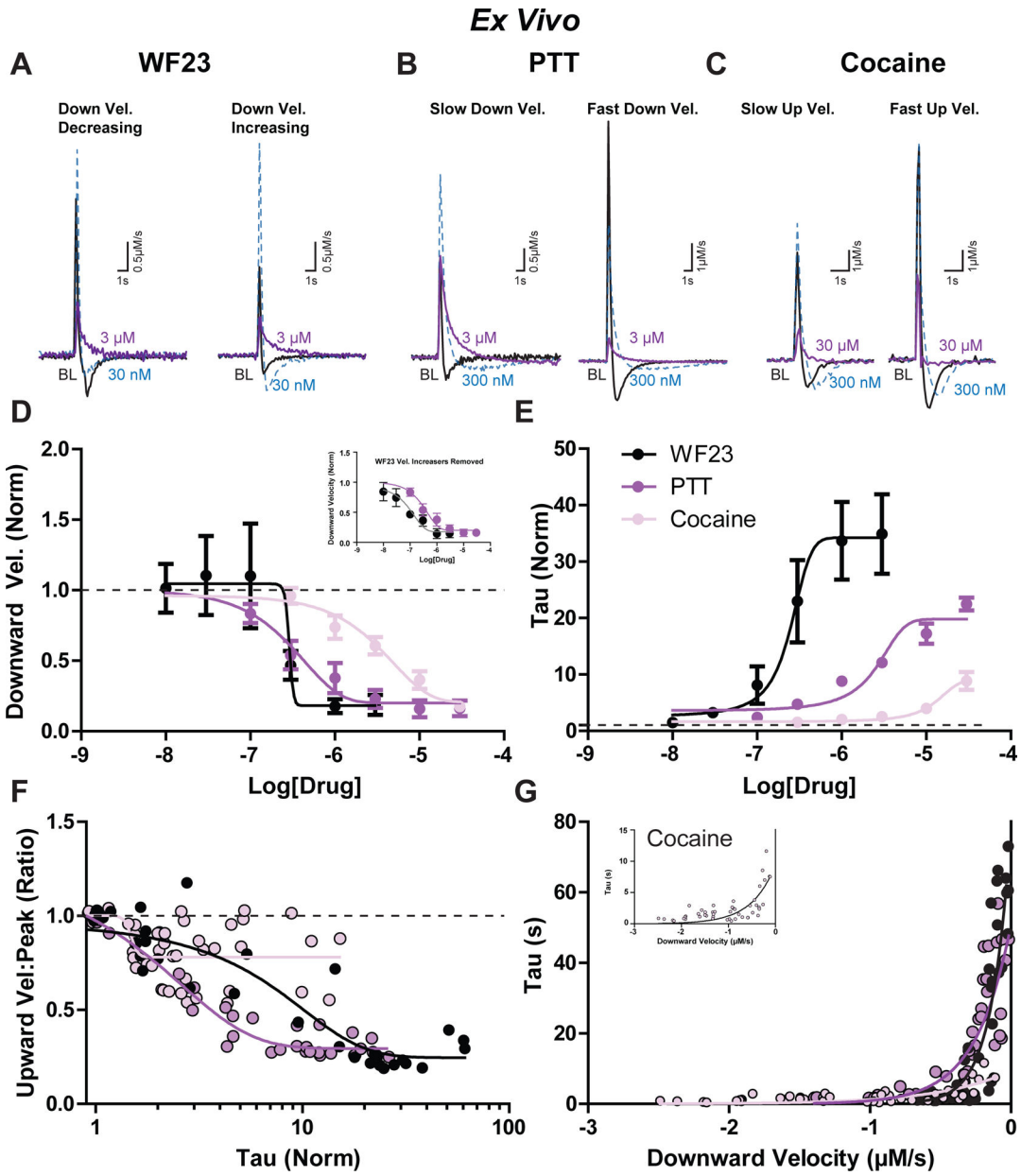

Figure 7. Effects of DAT blockers on dopamine uptake kinetics ex vivo

Example first derivative traces are shown under baseline conditions (black), 30 nM (blue), and 3 µM (purple) for A) WF23, B) PTT, and C) cocaine. A) three experiments indicated a distinct decrease in downward velocity with addition of WF23 at a low concentration (left) while in two experiments the downward velocity increased (right). B) experiments with slower downward velocity at baseline (left) are shown next to signals with faster downward velocity at baseline (right). C) experiments with slower upward velocity at baseline (left) are depicted next to signals with fast upward velocity at baseline (right). D) Downward velocity (normalized) and E) tau (normalized) are compared across increasing concentrations of WF23 (black), PTT (purple), and cocaine (pink). F) Relationship between tau (normalized)

and the ratio of upward velocity to peak height for each drug. G) Relationship between downward velocity (μM/s) and tau (sec) for each drug.

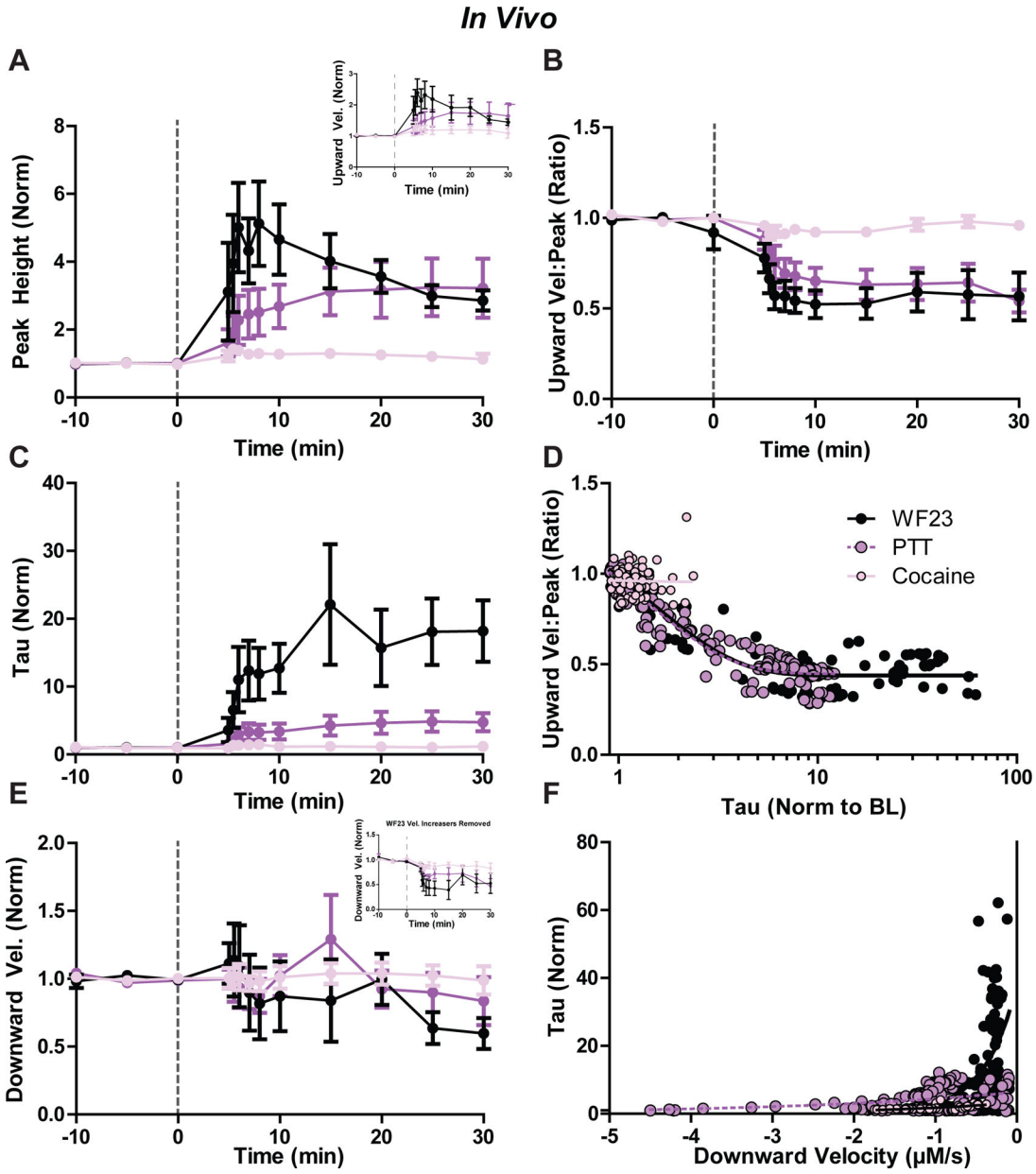

Figure 8. Effects of DAT blockers on dopamine release and uptake kinetics in vivo

Time course of psychostimulants on dopamine transmission across 30 minutes (post-injection) as measured by A) peak height, upward velocity (inset), B) ratio of upward velocity to peak height, C) exponential decay (tau), and E) downward velocity for WF23 (black), PTT (purple), and cocaine (pink). All values normalized to baseline. D) Comparison of tau (normalized) to ratio of upward velocity to peak height for each drug across the full time course. F) Comparison of downward velocity (normalized) to tau (normalized) for each drug.